

Available online at www.sciencedirect.com**SciVerse ScienceDirect**

Procedia Food Science 1 (2011) 1353 – 1358

Procedia
Food Science11th International Congress on Engineering and Food (ICEF11)

On flow-fields in a high pressure homogenizer and its implication on drop fragmentation

Andreas Håkansson^{a*}, Laszlo Fuchs^b, Fredrik Innings^c, Johan Revstedt^b,
Christian Trägårdh^a, Björn Bergenståhl^a

^a*Food Technology, Lund University, SE-226 46 Lund, Sweden*^b*Energy Sciences, Lund University, SE-226 46 Lund, Sweden*^c*Tetra Pak Processing Systems, SE-226 46 Lund, Sweden*

Abstract

The hydrodynamics of the High Pressure Homogenizer has been investigated in order to increase the understanding of the emulsification process. Fragmentation of drops in the homogenizer is generally assumed to be caused by cavitation and/or turbulence. Both processes are investigated experimentally in order to find its location in the HPH valve region. Cavitation was visualized by investigating light scattered in a HPH valve model with optical access. Detailed measurements of the one phase flow turbulence were obtained by Particle Image Velocimetry (PIV) on a carefully scaled model. The effects of dispersed phase flow volume fraction on the continuous phase turbulence was studied with refractive index matched PIV. The experiments show cavitation being focused in the first half of the gap whereas turbulence intensities are very low inside the gap. The turbulence is most effective in the outlet chamber downstream of the narrow gap. This is even more evident for the turbulent eddies of sizes comparable to the drops that are well known to be most efficient for the fragmentation. Increasing the disperse phase volume fraction does not alter the conclusion of highest turbulence downstream in the gap, however, it leads to an increase in energy of large turbulent eddies and a decrease in the energy of small scale eddies. This would imply a relative increase of the strength of the turbulent viscous mechanism compared to the turbulent inertial mechanism when increasing the volume fraction of dispersed phase. When comparing these findings on with visualizations of drop break-up; turbulence rather than cavitation seems to be the dominant mechanism of fragmentation in these geometries.

© 2011 Published by Elsevier B.V. Open access under [CC BY-NC-ND license](http://creativecommons.org/licenses/by-nc-nd/3.0/).

Selection and/or peer-review under responsibility of 11th International Congress on Engineering and Food (ICEF 11) Executive Committee.

Keywords: High pressure homogenization; Fragmentation; Turbulence; Cavitation; Emulsification.

* Corresponding author. Tel.: +46-46-2229670; fax: +46-46-2224622.

E-mail address: andreas.hakansson@food.lth.se.

1. Introduction

High pressure homogenization is widely used in the Food Industry for continuous production of emulsions-based foods (e.g. milk). Because of the high pressures (~ 10 -100 MPa), the energy consumption per volume is high. Furthermore, the energy utilized is extremely high if one compares to the theoretical energy needed for emulsification. Thus, the High Pressure Homogenizer (HPH) is a unit operation with large scale application and significant room for improvement by optimization.

A schematic view of the HPH valve region can be seen in Fig. 1. Pre-emulsion entering the valve is accelerated in the inlet chamber into the narrow ($h \sim 10$ -100 μm) gap and exits into the much larger outlet chamber.

The emulsification at low volume fractions of oil is largely controlled by the fragmentation process. Fragmentation of the disperse phase drops are driven by hydrodynamic forces; cavitation [1] and turbulence [2] for a large scale technical HPH.

Despite the fact that the HPH is an old process with wide application, the details of the fragmentation is still much unknown. Many experimental investigations focus on obtaining relations between operating conditions, such as homogenizing pressure and obtained Sauter mean diameter, viewing the entire emulsification process as a black-box model. Our hypothesis is that more fundamental knowledge on the emulsification process could be obtained by detailed investigation on the hydrodynamics of the process. The aim of this paper has been to investigate where in the homogenizer valve region cavitation and turbulence takes place and what this might infer on the mechanism(s) responsible for fragmentation.

The different hydrodynamic investigations in this study has been described individually in [3,4,5] and are here also discussed together with drop break-up visualization performed in the same geometries [6,7].

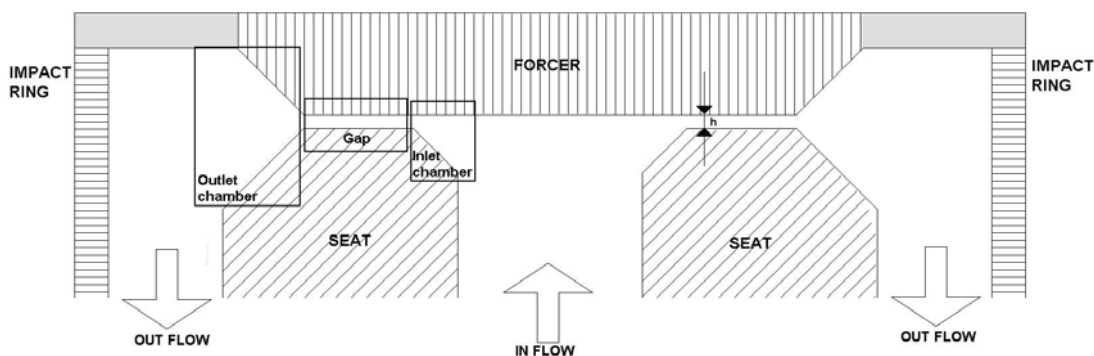


Fig. 1. Schematic (not to scale) view of the valve region in a technical High Pressure Homogenizer

2. Materials and Methods

Cavitation was visualized using a full scale cuboidal HPH valve with optical access developed by [6]. A CCD camera coupled to a microscope was used to take images of the flow. A pulse laser, entering the model at an angle orthogonal to the camera was used to illuminate the flow. Cavitation bubbles present in the flow would scatter laser light which can be detected with the camera. The investigations were run with degassed and filtered tap water seeded with nano particles for standardized nucleation. A more thorough description of the technique has been given elsewhere [3].

One-phase PIV was performed on a HPH valve scale model developed by [8]. Extension tubes and lenses were used to obtain a very small field of view and thus high resolution. Profiles of flow variables over the outlet chamber were obtained by compounding images over several camera positions. Details of the set-up and evaluation can be found elsewhere [4].

Two-phase PIV was performed on the same scale model using a model system of silica gel particles in an aqueous solution of sucrose and sodium chloride in order to obtain scaling of relevant dimensionless quantities and refractive index matching. Details of the set-up and evaluation can be found elsewhere [5].

3. Results and Discussion

Cavitation visualizations at an inlet pressure of 3 MPa can be seen in Fig. 2A, with flow entering from the top. Some weak scattering can be seen in the first half of the gap. Fig. 2B and 2C show micrographs with inlet pressures at 6 MPa and 8 MPa respectively. The scattering in the images can be seen to increase as a function of pressure. This was also tested by measuring cavitation noise by an ultra sound microphone. The sound intensity shows the same increase with pressure as the visualizations [3]. This is also consistent with previous measurements on HPH cavitation (e.g. [1]).

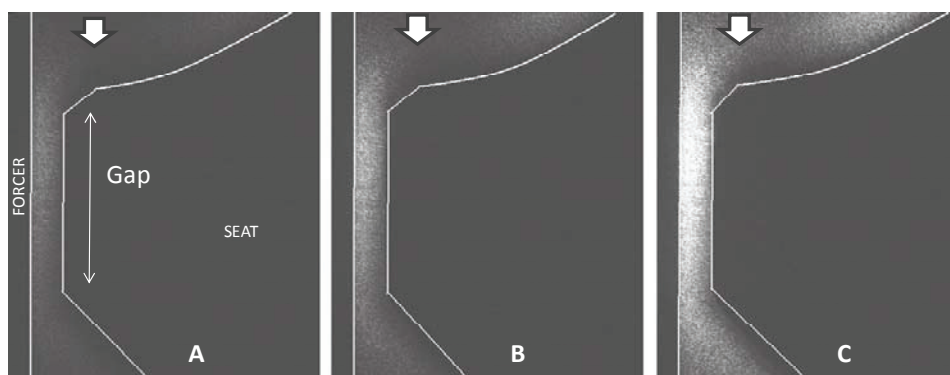


Fig. 2. Cavitation visualization in the gap region of a full scale homogenizer valve model. Inlet pressure (A) 3 MPa, (B) 6 MPa and (C) 8 MPa. (Atmospheric back-pressure)

The location of the scattering region is constant over pressures and at a maximum early in the gap. Some low intensity light scattering could also be seen upstream and downstream of the gap, however, this is most probably due to re-scattering in the gap material. For a more thorough discussion see [3]. The cavitation visualization thus implies cavitation bubbles to both expand and collapse inside the gap. This experimental finding is also consistent with theoretical calculations based on bubble-dynamics [3]. If the pressure shock wave would be responsible for oil drop fragmentation, break-up would consequently occur inside the gap. Drop fragmentation visualizations in the same model was performed in [6]. These investigations showed no fragmentation taking place inside the gap; instead, drops were fragmented further downstream in the outlet chamber. Some experimental differences do exist between the two experiments, e.g. the cavitation measurements used nano particles for controlling nucleation and no oil drops were present as in the visualization. These factors may change the extent of cavitation but would most likely only have a minor effect on the pressure profiles responsible for determining the location of cavitation.

Figure 3 show results for the velocity field measurements in the HPH. Fig 3A display mean velocity in the inlet chamber averaged over 400 images. The flow can be seen to accelerate into the narrow gap. Inside the gap, the flow follows a plug-flow velocity profile with a small degree of asymmetry due to the asymmetrical acceleration seen in Fig 3A. Turbulence is very low in the majority of the gap volume (turbulence intensity $\sim 1\%$) except close to the wall where, taking the mean velocity profile into account, only a low fraction of the drops will pass. Results for the gap flow and a more thorough discussion can be found in [4].

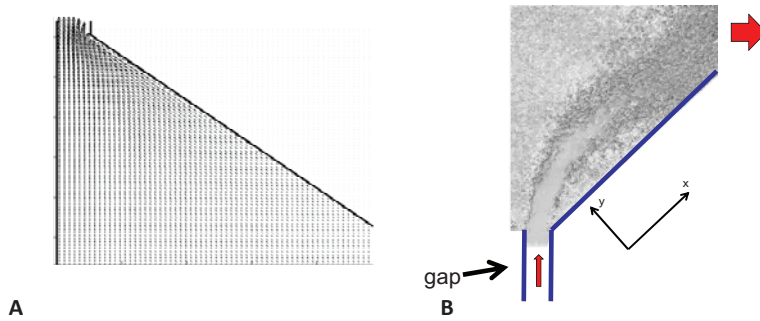


Fig. 3. A) Mean velocity field in the inlet chamber and B) instantaneous velocity vectors in outlet chamber

An instantaneous velocity field of the flow exiting the gap can be seen in Fig. 3B. The flow bends to the right and adheres to the right wall approximately 10 gap heights into the outlet chamber. This creates a circulatory motion in the major part of the outlet chamber as shown in [8]. The jet created in the outlet chamber is unsteady with high turbulence intensities. The streamwise Reynolds stress, $\langle uu \rangle$, over three lines at different downstream positions are shown in Fig. 4A. At the first position ($x = 2h$) the Reynolds stress is still very low in the centre of the gap but shows high values in the shear layers at the edges of the jet. Moving further downstream in the outlet chamber ($x = 8h$) the turbulence increases significantly as the mean velocity gradients continue to produce turbulence. The highest levels are still found in the shear layers although the relative difference is much smaller as turbulence is transported inwards towards the jet centre. Further downstream still ($x = 22h$) the turbulence decrease due to dissipation.

Fig. 4A shows that the turbulent kinetic energy is at a maximum close to 8 gap heights downstream of the gap. However, this is not necessarily the position where drops experience the highest level of turbulent fragmentation. A turbulent flow contains eddies of various sizes and $\langle uu \rangle$ is the total energy over all scales:

$$\langle uu \rangle = \int_0^{\infty} E_{11}(\kappa) d\kappa \quad (1)$$

where $E_{11}(\kappa)$ is the one dimensional turbulent kinetic energy spectra over wave number κ . It is well known that eddies of size comparable to the drop are most active in fragmenting it. For the Turbulent inertial mechanism of break-up the fragmenting force is best described by the energy of eddies smaller than the drop [2]:

$$\langle uu \rangle_d = \int_{2\pi/d}^{\infty} E_{11}(\kappa) d\kappa \quad (2)$$

One dimensional spectra was calculated based on the instantaneous velocity measurements and used to calculate $\langle uu \rangle_d$ over the three lines, the results can be seen in Fig. 4B based on a drop size obtained from scaling, see [4]. In comparison to the total, the small scale turbulence is highest furthest away from the gap. This is reasonable since energy is continuously transported towards smaller scales in the turbulent cascade. Another interesting observation is that $\langle uu \rangle_d$ still show clear peaks in the shear layers at $x = 22h$ whereas $\langle uu \rangle$ at this position is almost completely levelled out. Similar analysis of the turbulent viscous mechanism can be found in [4] and seem to imply maximum strength in the outlet chamber closer to $x = 8h$.

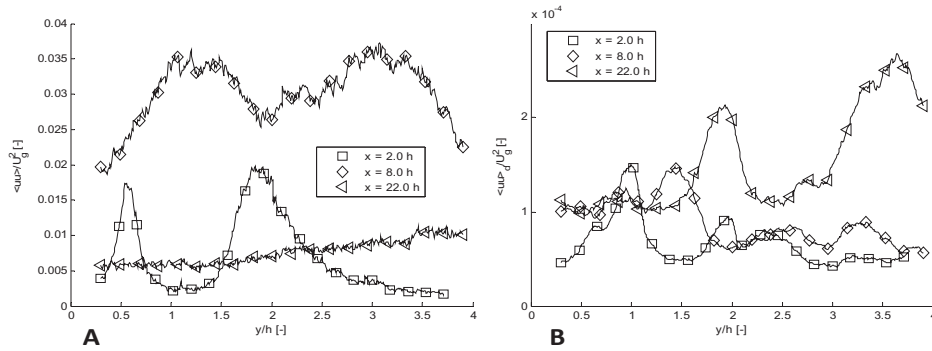


Fig. 4. A) Profiles of stream wise Reynolds stress, $\langle uu \rangle$, over three lines orthogonal to the right wall in Fig. 3B. (Fig. 8A in [4]), B) The small scale fluctuations calculated with Eq. 2. Note the differences in scale

Drop fragmentation visualizations in the same scale model show break-up taking place roughly between 10-20 gap height downstream and is thus consistent with fragmentation by turbulent forces. [7] The flow analysis in Fig. 2-4 was conducted in a one phase flow. It is well known that turbulence intensity and distribution over eddy length scale is altered by addition of disperse phase drops or particles, see e.g. [9]. PIV experiments were conducted at between 0.3% (v/v) and 3.3% (v/v) of disperse phase. Spectra of turbulent kinetic energy over eddy length scale can be seen in Fig. 5 with trends over concentrations indicated by arrows. The large scale eddies can be seen to increase in energy. Since most of the energy is contained in these large scales, the total energy, $\langle uu \rangle$, also increase with concentration. Based on the size of particles used in this experiments, an increase is also expected [9]. Simultaneously, the energy of small scale eddies decrease. This is an interesting finding since small scale eddies effect the drop by the inertial mechanism and the large eddies by a viscous mechanism [2]. Thus it seems as the relative importance of the viscous compared to the inertial mechanism increases with volume fraction of disperse phase.

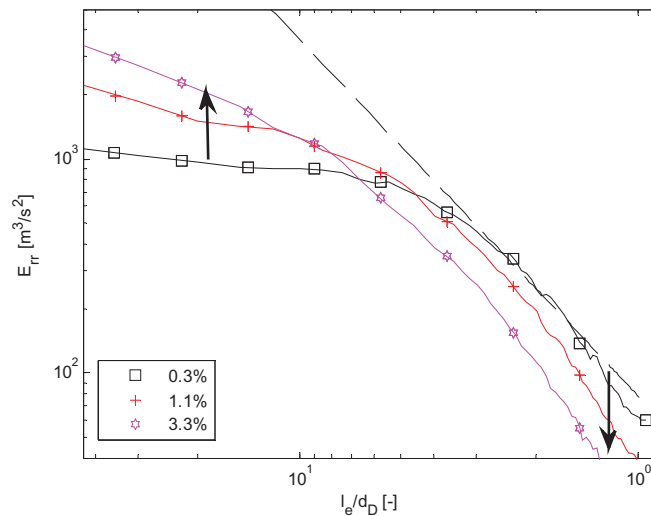


Fig. 5. Turbulent kinetic energy spectra for three volume fractions of disperse phase at the centre of the jet, $x = 9$ h. A dashed -5/3-slope line has been included for comparison. The arrows show the trend of shift in energy with concentration. Note the reversed scale on the horizontal axis

4. Conclusion

From an experimental investigation of the hydrodynamics of the HPH valve region it could be concluded that cavitation is found in the first half of the gap whereas turbulence is most effective in approximately 8-22 gap height downstream of the gap in the outlet chamber. When comparing to break-up visualizations this implies turbulence rather than cavitation being the dominating force for drop break-up. Investigation of turbulent energy over eddy length scale indicated a relative increase in the turbulent viscous mechanism to the turbulent inertial mechanism when increasing the volume fraction of dispersed phase.

Acknowledgements

This study was financed by the Swedish Research Council (VR).

References

- [1] Kurzthals H.-A. 1977. Untersuchungen über die physikalisch-technischen Vorgänge beim Homogenisieren von Milch in Hochdruck-Homogenisiermaschinen. Doctoral Thesis, Technischen Universität Hannover, Hannover, Germany.
- [2] Hinze J. 1955. Fundamentals of the Hydrodynamic Mechanism of Splitting in Dispersion Processes. *AIChE Journal*, 1(3), 289-295.
- [3] Håkansson A. Fuchs L. Innings F. Revstedt J. Bergenståhl B. & Trägårdh C. 2010. Visual Observation and acoustic measurements of cavitation in an experimental model of a high-pressure homogenizer. *Journal of Food Engineering* 100(3), 504-513.
- [4] Håkansson A. Fuchs L. Innings F. Revstedt J. Trägårdh C. & Bergenståhl B. 2011. High Resolution Experimental Measurement of Turbulent Flow Field in a High Pressure Homogenizer Model and its Implications on Turbulent Drop Fragmentation, *Chemical Engineering Science* 66(8), 1790-1801.
- [5] Håkansson A. Fuchs L. Innings F. Revstedt J. Trägårdh C. & Bergenståhl B. 2011. Turbulent Velocity Fields Measurements of Two Phase Flow in a High Pressure Homogenizer Scale Model. Submitted to journal.
- [6] Innings F. & Trägårdh C. 2005. Visualization of the Drop Deformation and Break-Up Process in a High Pressure Homogenizer. *Chemical Engineering Technology* 28(8), 882-891.
- [7] Innings, F. Fuchs L. & Trägårdh C. 2011 Theoretical and Experimental Analyses of Drop Deformation and Break-up in a Scale Model of a High-Pressure Homogenizer. *Journal of Food Engineering* 103(1), 21-28.
- [8] Innings F. & Trägårdh C. 2007. Analysis of the flow field in a high-pressure homogenizer, *Experimental Thermal and Fluid Science* 32(2), 345-354.
- [9] Roisman I.V. Oweis G.F. Ceccio S.L. Lyczkowski R. Troutt T.R. Mashayek F. Tsuji Y. Eaton J.K. Tropea C. & Matsumoto Y. 2006. Multiphase Interactions. In: Crowe C.T. (Ed.). *Multiphase Flow Handbook*. CRC Taylor & Francis, New York, New York, USA.

Presented at ICEF11 (May 22-26, 2011 – Athens, Greece) as paper AFT944.